of double $Ti_2(PO_4)_3$ units that share corner oxygen atoms, as shown in the slab structure in Figure 7. The slab structure is extended along the *ab* plane by interconnecting the double units through b-glide planes perpendicular to the *a* axis at $x = {}^1/_4$ and ${}^3/_4$. The top and bottom slabs are related by a c-glide plane, perpendicular to *b* at $y = {}^1/_4$ and ${}^3/_4$, and these parallel slabs are stacked along the *c* axis. The double units are connected so that two sizes of voids (3O + 3T and 4O + 4T) are found in a single slab plane. These cavities are centered by the cage lithium atoms, Li(1) and Li(2), respectively. Furthermore, the larger size void reflects the large isothermal ellipsoid found in Li(2), e.g. $B(eq) = 5$ (1) Å^2 (Table II).

Slab structures, having a similar perspective as the $x = 0.78$ phase in Figure 7, are shown for the $LiTi_2(PO_4)_3$ (Figure 8a, $x = 0.00$, NASICON structure) and the $Li_{2.72}Ti_2(PO_4)_3$ phases (Figure 8b, $x = 1.72$) for comparison. Obviously, the building blocks consist of PO_4 tetrahedra from adjacent slabs and infinite $[Ti_2(PO_4)_3]_\infty$ chains for the $x = 0.00$ phase, and single $Ti_2(PO_4)_3$ units for the $x = 1.72$ phase. All of these differences are believed to be associated with the composition of lithium and consequently the Ti^{3+}/Ti^{4+} cation distribution. This comparison illustrates the close relationship of NASICON to its structurally related compounds and yet, the apparent differences in the structures are not related by a simple distortion. Last, it is found that the number of large voids (characterized by 4O + 4T) decreases as the concentration of the lithium is increased. It would be interesting to see, then, how the ionic transport properties change as the number of larger voids is diminished. Experiments for the detailed conductivity measurements are planned.

Conclusion

Three solid solution regions in the $Li_{1+x}Ti_2(PO_4)_3$ series are observed, e.g., $0.00 \le x \le 0.50$ (I), $0.50 < x < 1.20$ (II), and $1.20 \le x \le 2.00$ (III). Regions I, II, and III represent the extended solid solutions of the above mentioned $x = 0.00$ (NASICON structure), 0.78 and 1.72 ($Sc_2(WO_4)_3$ type) phases, respectively. X-ray single-crystal structure studies for the $x = 0.78$ phase have shown an original structure that is closely related to the NASICON structure. The solid solution series $Li_{1+x}Ti_2(PO_4)_3$ and the crystal structures of the $x = 0.78$ and 1.72 phases provide an integrated system for the systematic study of the relationship between ionic conductivity and framework structures (including phase transformation, cavity geometry, etc.).

Acknowledgment is made to the National Science Foundation, Solid State Chemistry (SGER, Grant DMR-9012983), and the donors of the Petroleum Research Fund, administered by the American Chemical Society for support of this research. Financial support for the single-crystal X-ray diffractometer by the National Science Foundation is gratefully acknowledged. The authors are indebted to Professor D. Calahan for scanning electron microscopy photographs.

Registry No. $Li_{1-3}Ti_2(PO_4)_3$, 119536-20-8; $Li_{1.78}Ti_2(PO_4)_3$, 140225-42-9; $LiTi_2(PO_4)_3$, 30622-39-0; $Li_{2.72}Ti_2(PO_4)_3$, 119536-22-0.

Supplementary Material Available: Table SI listing anisotropic thermal parameters and Table SII listing refined lattice parameters for polycrystalline $Li_{1+x}Ti_2(PO_4)_3$, $0.00 \le x \le 2.00$ (2 pages); Table SIII, observed and calculated structure factors (11 pages). Ordering information is given on any current masthead page.

Preparation, Solid-State Characterization, and Surface Chemistry of High Surface Area $Ni_xAl_{2-2x}O_{3-2x}$ Mixed Oxides

Guido Busca,* Vincenzo Lorenzelli, and Vicente Sanchez Escribano†

Istituto di Chimica, Facoltà di Ingegneria, Università di Genova P.le Kennedy, I-16129 Genova, Italy

Received October 9, 1991. Revised Manuscript Received January 23, 1992

High surface area $Ni_xAl_{2-2x}O_{3-2x}$ oxides have been prepared ($x = 0$, 0.33, 0.44, 0.5, 0.66, 0.85, 1) by a coprecipitation procedure. Both the precipitates and the calcined materials have been characterized structurally by XRD, FT-IR, and TG-DTG analyses. The precipitates are constituted by boehmite ($x = 0$), by amorphous hydroxy nitrates ($x = 0.33$, 0.44, and 0.5), by a mixed hydroxy-nitrate similar to Takovite ($x = 0.66$), and by the compound $Ni_6Al_2CO_3(OH)_{16}\cdot 4H_2O$, the Ni analogue of hydrotalcite, for $x = 0.85$. The calcined mixed oxides are constituted by the spinel type compounds γ-Al_2O_3 and $NiAl_2O_4$ and their solid solutions for $0 \le x \le 0.5$, while for $x = 0.85$ a rock salt type NiO phase containing Al^{3+} in both tetrahedral and octahedral sites is obtained. For $x = 0.66$ a mixture of the spinel and the rock salt type phase is found. The porosity and the surface structure of the calcined $Ni_xAl_{2-2x}O_{3-x}$ mixed oxides have been investigated by liquid nitrogen adsorption and FT-IR spectroscopy of surface hydroxy group and of adsorbed carbon monoxide and pyridine. The surface composition of these materials, all mesoporous, reflects their bulk structure. Cation vacancy clusters in defective spinels ($x < 0.5$) are responsible for characteristic surface structures. The presence of Al^{3+} in the bulk of rock salt type NiO (sample with $x = 0.85$) results in a deep modification of its acid-base and electronic properties. Precipitation with Na_2CO_3 instead of $(NH_4)_2CO_3$ produces $NiAl_2O_4$, whose surface chemical properties are modified by Na^+ contamination.

Introduction

High surface area homogeneous mixed oxide powders find a number of industrial applications (i.e., in catalysis, adsorption, pigment, sensor, and magnetic technologies[1-4]). To obtain these powders, preparation techniques allowing an intimate mixture of the component ions without high-temperature treatments must be employed. Coprecipitation methods, consisting of the precipitation of mixed hydroxides, hydroxy carbonates or hydroxy nitrates from

† On leave from Departamento de Quimica Inorganica, Facultad de Ciencias Quimicas, Universidad de Salamanca, Spain.

(1) Dadyburior, D. D.; Jewur, S. S.; Ruckenstein, E. *Catal. Rev. Sci. Eng.* **1979**, *19*, 293.
(2) Lew, S.; Jothimurugesan, K.; Flytzani-Stephanopulos, M. *Ind. Chem. Res.* **1989**, *28*, 535.
(3) Shimizu, Y.; Arai, H.; Seiyama, *Sensors Actuators* **1985**, *7*, 11.
(4) Suresh, K.; Kumar, N. R. S.; Patil, K. C. *Adv. Mater.* **1991**, *3*, 148.

0897-4756/92/2804-0595$03.00/0

Table I. Summary of Characteristics of $Ni_xAl_{2-2x}O_{3-2x}$ Mixed Oxides

notation	dried precipitate XRD phase	calcined mixed oxides: Ni/Ni + Al ar x	Ni/Ni + Al ar nomin	Ni/Ni + Al ar meas	XRD data phase	cryst size[a]	surface area[b]	pore str V^c	pore str r^d
Ni000	bohemite	0	0.00	0.0	γ-Al_2O_3	15.3	97.6	0.23	9.3
Ni033	amorphous	0.33	0.20	0.18	spinel	24.5	108.0	0.23	8.6
Ni044	amorphous	0.44	0.29		spinel	17.1	122.0		
Ni050	amorphous	0.50	0.33	0.36	$NiAl_2O_4$	20.3	132.9	0.21	6.2
Ni050Na	amorphous	0.50	0.33	0.28	$NiAl_2O_4$(+NiO)		127.7	0.28	8.8
Ni066	takovite	0.69	0.50		spinel + NiO		120.0		
Ni085	hydrotalcite-like	0.85	0.75	0.74	NiO-like	20.2	110.5	0.23	8.2
Ni100	amorphous	1.00	1.00	1.00	NiO	32.3	82.0	0.16	7.7

[a] Measured from the 440 diffraction peak of spinels and from the corresponding 220 peak of rock-salt, nm. [b] m^2/g. [c] Pore volume, mL/g. [d] Medium proe radius, nm.

water solutions of mixed salts, followed by thermal decomposition at moderate temperatures, fulfill these requirements. Monophasic ternary oxides (such as spinels,[5,6] perovskites,[7] etc.) as well as solid solutions[6] can be prepared in such a way, although frequently polyphasic materials are obtained.

High surface area mixed Ni–Al oxides with varying Ni/Al ratios find applications as precursors of catalysts for methane steam re-forming[8] and in the pigment industry.[9] They have also been reported to be excellent catalysts for olefin nitroxidation[10] and for the catalytic combustion of volatile organics.[11] Ni-deficient aluminate spinels can also have a role in petroleum hydrotreating catalysis, carried out over sulfided Ni–W/Al_2O_3 and Ni–Mo/Al_2O_3 catalysts.[12] While several papers have been published describing the preparation chemistry of high nickel content precipitates and their transformation into reduced Ni metal catalysts,[8,13] much less is known about the intermediate oxides or about the preparation and structure of high aluminum content materials.[14] Moreover, the surface chemistry of the nonstoichiometric Ni–Al mixed oxides was never investigated previously, to our knowledge. Only a few data can be found on the surface chemistry of the stoichiometric compound $NiAl_2O_4$.[15–17]

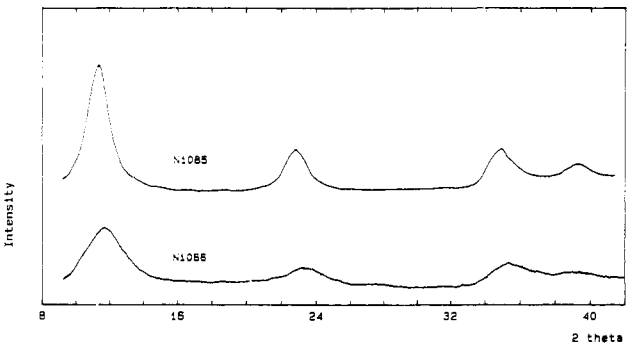

Figure 1. XRD patterns (Cu Kα radiation) of the precipitates Ni066 and Ni085.

Table II. X-ray Diffraction Peaks (d, Å) for Mixed Ni–Al Precipitates and Related Compounds

takovite[a]	Ni066	Ni085	hydrotalcite[b]	reevesite[c]
7.57	7.56	7.85	7.84	7.63
3.77	3.83	3.90	3.90	3.80
2.552	2.50	2.58	2.60	2.60
2.264	2.30	2.30	2.33	2.30
1.917		1.96	1.990	1.946
1.510	1.50	1.52	1.541	1.537
1.481		1.50	1.498	1.508

[a] JCPDS table 15-87; $Ni_5Al_4O_2(OH)_{18}\cdot 6H_2O$. [b] JCPDS table 22-700; $Mg_6Al_2CO_3(OH)_{16}\cdot 4H_2O$. [c] JCPDS table 20-786; $Ni_6Fe_2CO_3(OH)_{16}\cdot 4H_2O$.

The structure of the mixed oxide $NiAl_2O_4$ (an inverse spinel[18]) is related to those of the pure oxides NiO and γ-Al_2O_3 due to the common cubic close packed array of oxide ions. According to the strong stabilization energy for octahedral coordination, Ni^{2+} occupies octahedral sites in the rock salt like compound NiO and, predominatly, also in the inverse spinel $NiAl_2O_4$, while aluminum ions are distributed between octahedral and tetrahedral sites in both transitional aluminas (namely on the γ phase[19]) and in the inverse spinels. The present paper summarizes our work on the preparation of high surface area $Ni_xAl_{2-2x}O_{3-2x}$ mixed oxides taking into account all compositional range ($0 \le x \le 1$) and on the characterization of their structure and phase composition as well as of their surface chemistry.

Experimental Section

(a) Preparation Method. The precursor powders have been prepared by coprecipitation at pH = 8 from mixed water solutions of $Ni(NO_3)_2\cdot 6H_2O$ and $Al(NO_3)_3\cdot 9H_2O$ by addition of $(NH_4)_2CO_3$.

(5) Di Conca, M.; Riva, A.; Trifirò, F.; Vaccari, A.; Del Piero, G.; Fattore, V.; Pincolini, F. *Proc. 8th Int. Congr. Catalysis*; Verlag Chemie: Berlin, 1984; Vol. 2, p 173.
(6) Busca, G.; Trifirò, F.; Vaccari, A. *Langmuir* **1990**, *6*, 1440.
(7) Tejuca, L. G.; Fierro, J. L. G.; Tascon, J. M. D. *Adv. Catal.* **1989**, *36*, 237.
(8) (a) Rostrup-Nielsen, J. R. *Steam Reforming Catalysts*; Teknisk Forlag: Copenhagen, 1975. (b) Twigg, M. V., Ed. *Catalyst Handbook*; Wolfe Publishers: London, 1989.
(9) Buchner, W.; Schliebs, R.; Winter, G.; Buchel, K. H. *Industrial Inorganic Chemistry*; VCH: Weinheim, Germany, 1989.
(10) Pajonk, G. M. In *New Developments in selective oxidation*; Trifirò, F., Centi, G., Eds.; Elsevier: Amsterdam, 1990; p 229.
(11) Ozkan, U. S.; Kueller R. F.; Monteczuma, E. *Ind. Eng. Chem. Res.* **1990**, *29*, 1136.
(12) (a) Speight, J. G. *The Chemistry and Technology of Petroleum*, 2nd ed.; Marcel Dekker: New York, 1991. (b) Trimm, D. L.; Akashah, S.; Absi-Halabi, M.; Bishara, A. *Catalysts in Petroleum Refining 1989*; Elsevier: Amsterdam, 1990. (c) Ledoux, M. J. In *Catalysis*; Bond, G. C., Webb, G., Eds.; The Royal Society of Chemistry: London, 1985; Vol. 7, p 125.
(13) (a) Longuet-Escard, J. *J. Chim. Phys.* **1950**, *47*, *238*. (b) Kruissink, E. C.; VanReijen, L. L.; Ross, J. R. H. *J. Chem. Soc., Faraday Trans. 1* **1981**, *77*, 649. (c) Alzamora, L. E.; Ross, J. R. H.; Kruissink, E. C.; VanReijen, L. L. *J. Chem. Soc., Faraday Trans. 1* **1981**, *77*, 665. (d) Puxley, D. C.; Kitchener, I. J.; Komodromos, C.; Parkyns, N. D. In *Preparation of Catalysts III*; Poncelet, G., et al., Eds.; Elsevier: Amsterdam, 1983; p 237. (e) Hernandez, M. J.; Ulibarri, M. A.; Rendon, J. L.; Serna, C. J. *Thermochim. Acta* **1984**, *81*, 311. (f) Ross, J. R. H. In *Catalysis*; The Royal Society of Chemistry: London, 1985; Vol. 7, p 1. (g) Gadalla, A. H.; Sommer, M. E. *J. Am. Ceram. Soc.* **1989**, *72*, 683. (h) Clause, O.; Gazzano, M.; Trifirò, F.; Vaccari, A.; Zatorski, L. *Appl. Catal.* **1991**, *73*, 217.
(14) (a) Milligan, W. O.; Merten, L. *J. Phys. Chem.* **1946**, *50*, 465. (b) Akimov, V. M.; Slinkin, A. A.; Kretalova, L. D. Rubinshtein, A. M. *Bull. Acad. Sci. USSR, Div. Chim. Sci.* **1960**, *4*, 624. (c) Levina, V. V.; Danyushevskii, V. Y.; Boevskaya, E. A.; Kapustin, G. I.; Yakerson, V. I. *Bull. Acad. Sci. USSR Chem. J.* **1975**, *918*, 2533.
(15) Lo Jacono, M.; Schiavello, M.; Cimino, A. *J. Phys. Chem.* **1971**, *75*, 1044.
(16) Shelef, M.; Wheeler, M. A. Z.; Yao, H. C. *Surf. Sci.* **1975**, *47*, 697.
(17) Busca, G.; Lorenzelli, V.; Sanchez Escribano, V.; Guidetti, R. *J. Catal.* **1991**, *131*, 167.
(18) Mocala, K.; Navrotski, A. *J. Am. Ceram. Soc.* **1989**, *72*, 826.
(19) Wilson, S. J.; McConnell, J. D. C. *J. Solid State Chem.* **1980**, *34*, 315.

After filtering, the precipitates have been washed carefully and dried at 390 K for 3 h. The mixed oxides have been produced by calcination in air of the precursors at 1073 K for 3 h. One more sample is considered in this paper, having a nominal composition corresponding to the formula $NiAl_2O_4$, obtained by the same procedure but using Na_2CO_3 instead of $(NH_4)_2CO_3$ as the precipitating agent. All reagents were from Carlo Erba (Milano, Italy).

(b) Characterization Procedures. TG and XRD analyses have been performed with Setaram Model 92/19 and Philips Model PW 1130-1049/10 (Cu Kα radiation) instruments, respectively.

The elemental analysis has been carried out by a Plasma II Perkin-Elmer emission spectrometer after dissolution in a HF/HNO_3 mixture.

Microstructural characterization was done by nitrogen adsorption at 77 K using a conventional volumetric apparatus.[20,21] The IR spectra were recorded by a Nicolet MX1 Fourier transform instrument, using a liquid nitrogen cooled cell connected to conventional gas-handling system. The carbon monoxide was from SIO (Milano, Italy), and pyridine was from Carbo Erba (Milano, Italy).

Results and Discussion

(a) Characterization of Precipitates. Some properties of the materials under study are summarized in Table I. The materials will be denoted hereonafter by the value of x referred to the nominal stoichiometry $Ni_xAl_{2-2x}O_{3-2x}$ of the calcined materials. The correspondence of the real compositions with the nominal ones has been checked on some calcined materials by elemental analysis. The results, also reported in Table I, show that the real compositions closely correspond to the nominal ones.

The precipitated materials for x = 0.33, 0.44, and 0.5 appear amorphous in XRD analysis. The XRD pattern for the precipitate Ni000 is completely consistent with that reported for Boehmite (γ-AlOOH[22]). In Figure 1 the XRD patterns of the Ni066 and Ni085 precipitates are shown. In Table II the peak position observed in the XRD spectra of Ni066 and Ni085 precipitates are compared with those reported in the literature for three structurally related compounds, the minerals takovite, a layered Ni–Al mixed hydroxide, and hydrotalcite and reevesite, isostructural Mg^{2+}/Al^{3+} and Ni^{2+}/Fe^{3+} hydroxy carbonates. It is evident that the patterns are all similar, due to the closely related structures of these materials. The XRD spectrum of our Ni085 precursor is very similar to those of reevesite and hydrotalcite, according to the same bivalent metal/trivalent metal atomic ratio, and to the similar size of Ni^{2+} and Mg^{2+} ions (0.70 and 0.72, respectively, for octahedral coordination[23]). Similar Ni–Al precipitates have been characterized previously.[13] The pattern of Ni066 resembles that of takovite, in spite of the slightly different Ni/Al atomic ratio. Taking into account the series Ni066, takovite, and Ni085, relevant shifts of the diffraction peaks are observed, certainly related to the increasing Ni:Al ratios of the materials (50:50 for Ni066; 55:45 for takovite; 75:25 for Ni085). Indeed the cell parameters seem to vary regularly in relation with this ratio, as already shown by other authors.[13]

The IR spectra of the precipitates are compared in Figure 2. Again the spectrum of the Ni000 precipitate agrees with that reported for boehmite,[24] although carbonate and nitrate species are also present, at the impurity level. The spectra of the amorphous precipitates Ni033, Ni044, and Ni050 and of Ni066 are similar to each other and show very prominently the features of almost symmetrical nitrate species (sharp bands at 1390 cm^{-1}, very strong, and 830 cm^{-1}, weak, due to the NO asymmetric stretching and in-plane deformation, respectively) and of carbonate species, characterized by the broad asymmetric CO stretching near 1400 cm^{-1}. Bands in the region 1200–1000 cm^{-1} (OH deformation bands) indicate that relatively strong H bondings are present in these mixed precipitates, suggesting that these materials are mainly constituted of Ni–Al hydroxy compounds. The position of the most intense bands in the region 400–600 cm^{-1} (detected near 620 and 480 cm^{-1} in boehmite, and near 550 and 430 cm^{-1} in the mixed precipitates) should be the result of the presence of condensed NiO_6 and AlO_6 octahedra.

Table III. Observed Wavenumbers (cm^{-1}) of the IR Spectra of the Precipitate Ni085 and of the Mineral Hydrotalcite

Ni085	hydrotalcite[a]	Ni085	hydrotalcite[a]
3500	3575	850 sh	865 sh
1650 br	1650 w, br	750 vs	
1530 br	1520 sh	590 vs	650 vs
1380 ms	1400 m	560	
1050 sh		419 vs	412 vs

[a] Reference 25.

Table IV. Weight Loss upon Calcination of Ni–Al Coprecipitates

notation	weight loss, %	notation	weight loss, %
Ni033	51.6	Ni066	38.4
Ni044	49.0	Ni085	36.8
Ni050	39.6		

The positions of the observed bands for Ni085 are compared in Table III with those of the spectrum reported in the literature for hydrotalcite.[25] By taking into account the substitution of Ni^{2+} for Mg^{2+}, the spectra appear indeed very similar. So, both IR and XRD analyses strongly suggest the identification of the Ni085 precipitate as the compound $Ni_6Al_2(OH)_{16}(CO_3)\cdot 4H_2O$, the Ni analogue of hydrotalcite. This compound is a member of a family of structure-related compounds including also takovite, having a layered structure derived from that of the brucite-type bivalent metal hydroxides such as brucite ($Mg(OH)_2$) and $Ni(OH)_2$. In these compounds some bivalent ions in the hydroxide layer are replaced by trivalent ones: so, an excess of catonic charge on the layers is produced, that is balanced by anions (carbonates and/or nitrates) in the interlayer region, where also water molecules can be located.

In Figure 3 the TG-DTG curves relative to the calcination of the Ni–Al mixed precipitates are shown. Three stages are evident in the DTG curves of all Ni-containing materials, although the first one, occurring near 420 K, is likely related to desorption of adsorbed contaminants, mainly water. Apparently, two steps follow. They fall in the ranges 520–570 K and near 690 K. The relative weight of the two peaks, however, inverts progressively, the importance of the last peak growing with increasing x following the sequence Ni033 < Ni050 < Ni066 < Ni085. Decomposition is complete below 770 K, for all mixed compounds.

The total weight loss upon thermal decomposition of the precipitates is also sensitive to the composition, as shown

(20) Pierce, C. *J. Phys. Chem.* **1953**, *57*, 149.
(21) Orr, C.; Dallavalle, J. M. *Fine Particle Measurement*; McMillan: New York, 1959; p 271.
(22) Lippens, B. C.; Staggerda, J. J. In *Physical and Chemical Aspects of Adsorption and Catalysis*; Linsen, B. G., Ed.; Academic Press: New York, 1970; p 171.
(23) Moeller, T. *Inorganic Chemistry*; Wiley: New York, 1982; p 141.
(24) Stegmann, M. C.; Vivien, D.; Mazieres, C. *Spectrochim. Acta* **1973**, *29A*, 1653.
(25) Gadsden, J. A. *Infrared Spectra of Minerals and Related Inorganic Compounds*; Butterworths: London, 1975.

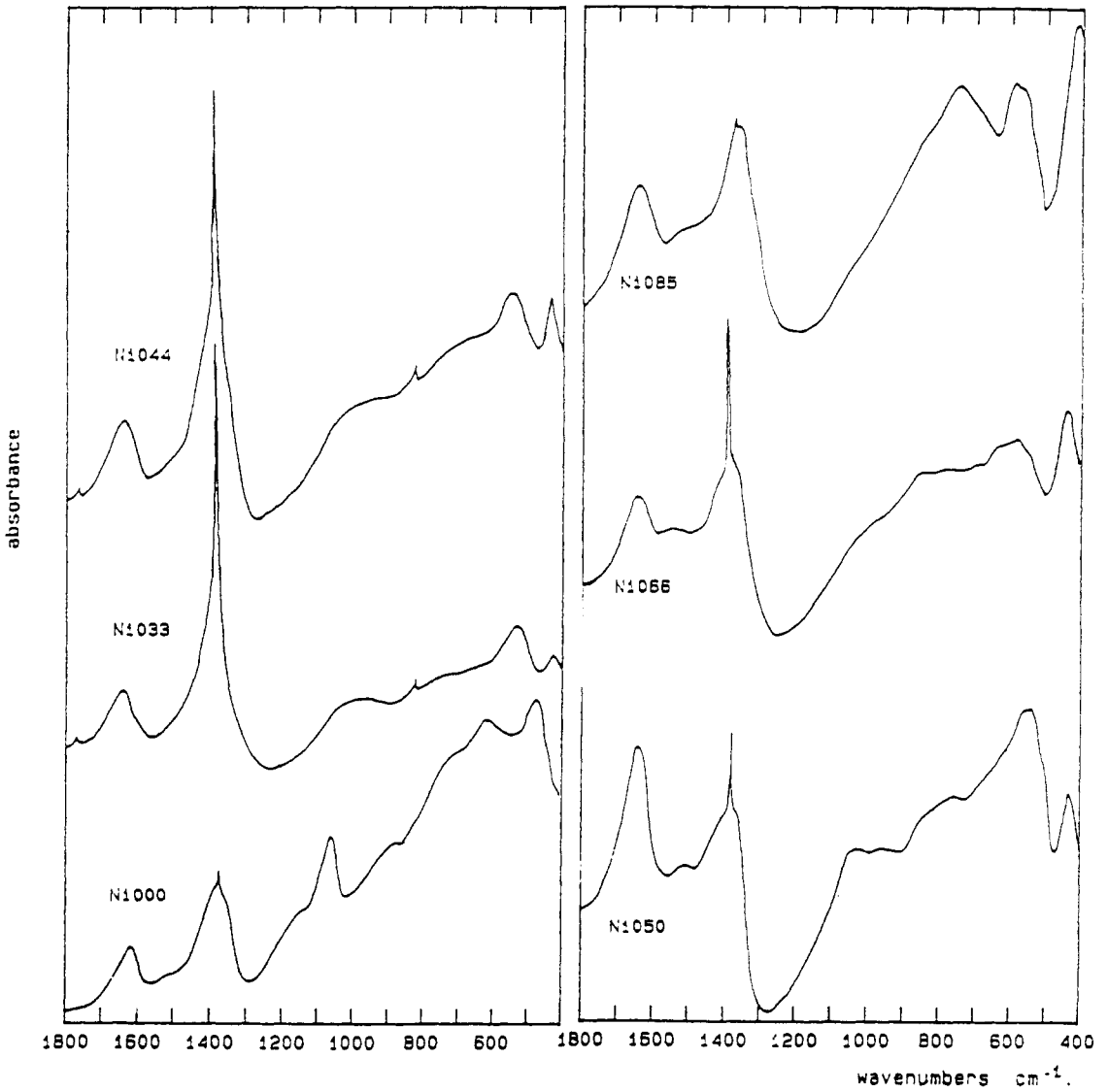

Figure 2. IR spectra (KBr pressed disks) of the Ni–Al mixed precipitates.

in Table IV. The weight loss for the sample Ni085 accords to the theoretical one forecast for the compound $Ni_6Al_2(OH)_{16}(CO_3)\cdot 4H_2O$, (32.1%). In fact, the deconvolution of the DTG curve suggests that the first step, likely mainly related to desorption of surface water, accounts for near 7% of the total weight. The successive two steps (32.2% of the remaining material), account for 8.6% and 23.5% of the compound weight, respectively. It seems reasonable to propose that our compound first loses its four interlayer water molecules (theoretical loss 8.9%) and then decomposes to the oxide (theoretical loss 23.2%). This behavior is similar to that reported for hydrotalcite.[26] So, also TG-DTG data support the above composition and the identification of Ni085 as the Ni analogue of hydrotalcite.

The weight loss in the case of the precipitate Ni066, if the first step is subtracted, is only slightly higher than the theoretical one calculated for takovite, while it grows further by increasing Al content. This can be related to the presence of higher amounts of crystallization water in these mixed hydroxy nitrates.

(b) Bulk Characterization of Calcined Materials. The XRD spectra of the samples characterized by $x < 0.5$ (Figure 4) correspond to monophasic spinel-type compounds. Only in the case of Ni050 (Figures 4 and 5) together with the pattern of the inverse spinel $NiAl_2O_4$,[18] weak features are also detected relative to a rock salt type phase. These features are only slightly stronger in the spectrum of the sample Ni050Na. The pattern of the sample Ni000 closely corresponds to that of γ-Al_2O_3,[19,22] whose structure is that of a cation-deficient spinel, while those of Ni033 and Ni044 are intermediate between those of the two above structures. The peaks, whose position is reported in Table V, shift progressively, evidencing a progressive expansion of the cubic cell from γ-Al_2O_3 to $NiAl_2O_4$. This points to that Ni033 and Ni044 materials are Ni-deficient spinels, so being solid solutions of γ-Al_2O_3 and $NiAl_2O_4$. The possibility of these solutions was already shown for high-temperature treated materials by Lefebvre et al.[27] A similar solubility with the formation of nonstoichiometric spinels was already reported in the case of Al_2O_3–$MgAl_2O_4$,[28,29] although in these cases a normal spinel is involved.

The XRD pattern of the compound Ni066 shows that this is definitely a biphasic material (Figure 5). The spinel pattern is in fact well discernible and, almost surprisingly,

(26) Gastuche, K. C.; Brown, G.; Mortland, M. M. *Clay Mineral.* **1967**, *7*, 177.

(27) Lefebvre, A.; Gilles, J. C.; Collongues, R. *C.R. Acad. Sci. Paris, Ser. C* **1971**, *273*, 61.

(28) Bhattacharya, H.; Sammadar, B. N. *J. Am. Ceram. Soc.* **1978**, *61*, 279.

(29) Kiang, Yet Ming; Kingery, W. D. *J. Am. Ceram. Soc.* **1989**, *72*, 271.

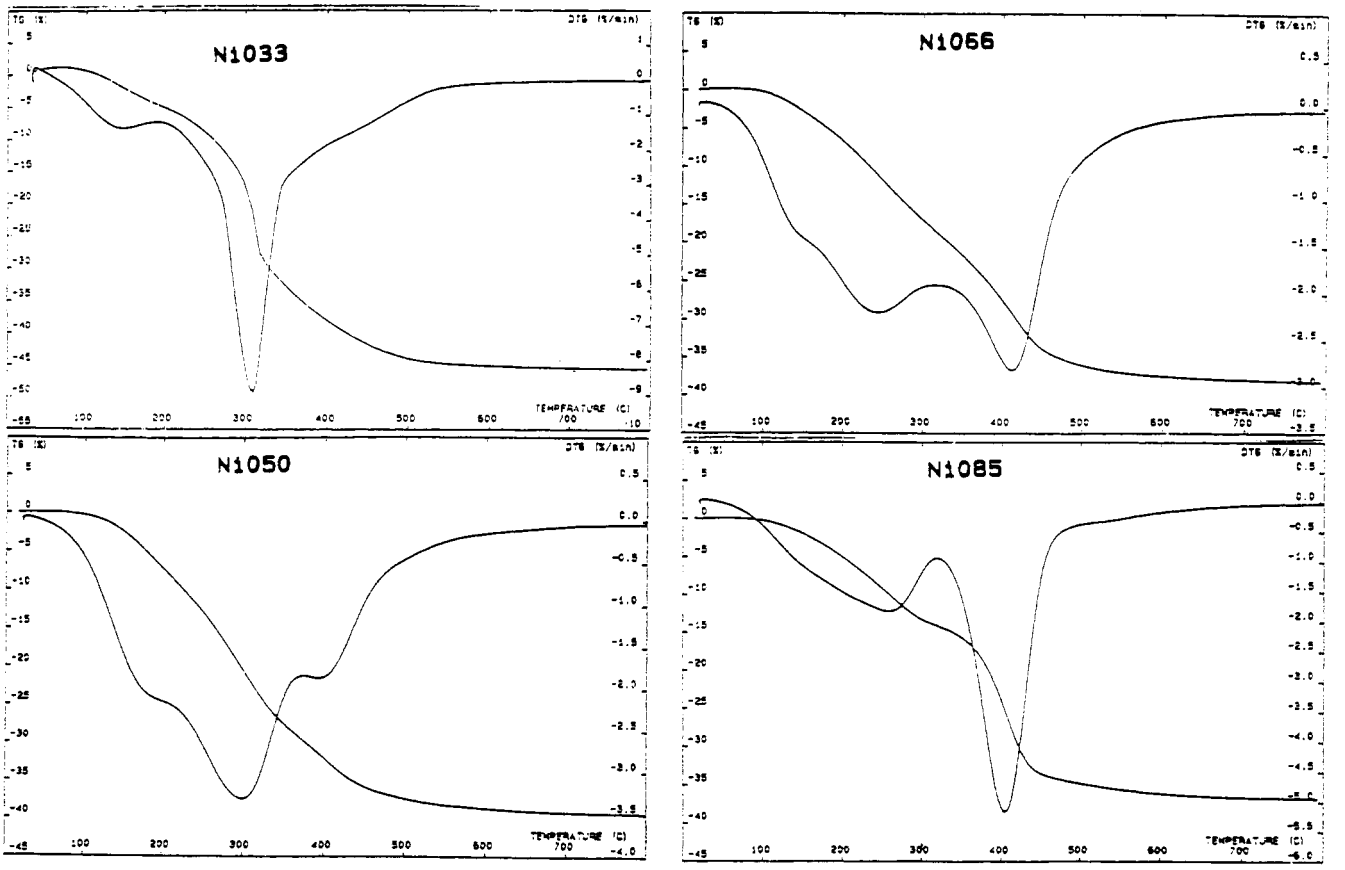

Figure 3. TG-DTG curves relative to the thermal decomposition of Ni–Al mixed precipitates.

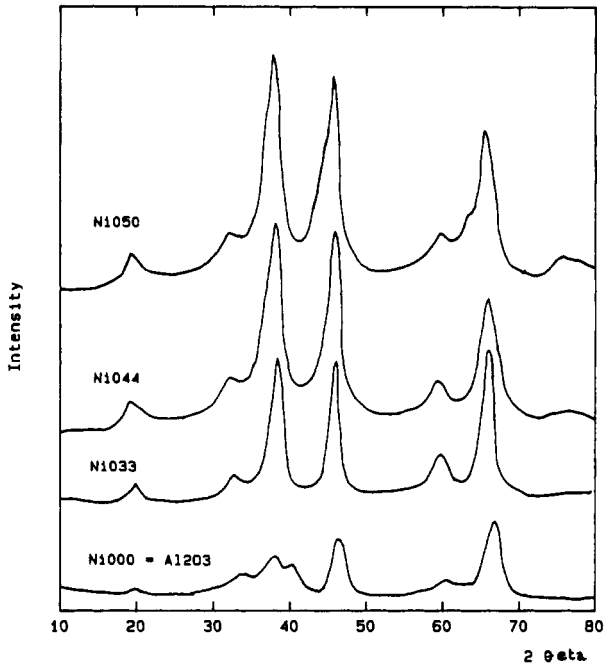

Figure 4. XRD patterns of the Ni000, Ni033, Ni044, and Ni050 calcined powders.

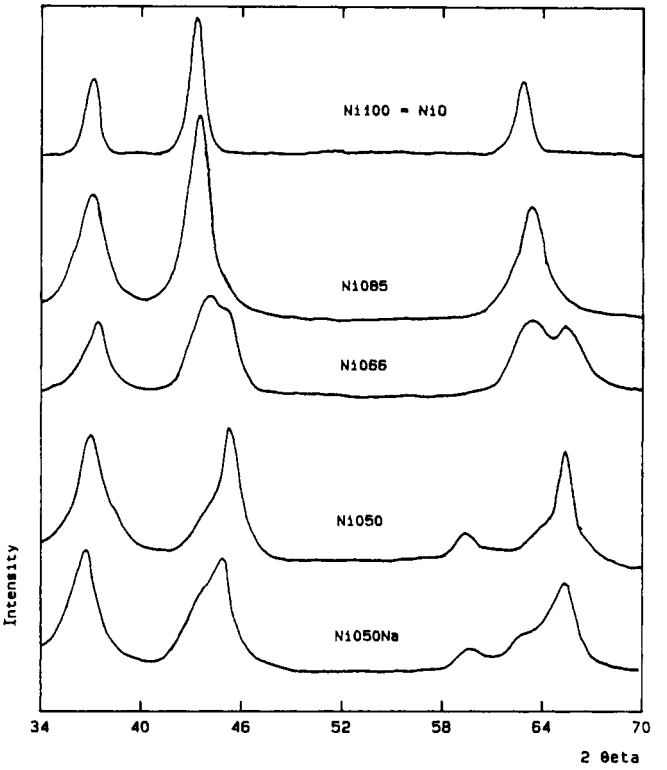

Figure 5. XRD patterns of the Ni050Na, Ni050, Ni066, Ni085, and Ni100 calcined powders.

should correspond to a Ni-deficient spinel phase (see the peak position in Table V). Onto this pattern, another one typical for a rock-salt type phase is superimposed. On the contrary, the Ni085 material is again a monophasic one: its XRD spectrum is of the rock-salt type, strongly related to that of NiO. A careful analysis of the shape of its XRD peaks (Figure 5) seems to be sufficient to exclude the presence of significant amounts of the spinel phase. However, the data reported in Table V show that the cell peaks of this phase are significantly shifted with respect to those of pure NiO, this shift being dependent on the Al content in the preparation. This phase, already reported by other authors,[13] is "isolated" in the sample Ni085.

To have further microscopic data on the solid state of the calcined materials, their IR spectra have also been

Table V. XRD Patterns of $Ni_xAl_{2-2x}O_{3-2x}$ Mixed Oxides and of Reference Compounds (d, Å)

$Ni_xAl_{2-2x}O_{3-2x}$ mixed oxides							γ-Al_2O_3[a]		$NiAl_2O_4$[b]		NiO[c]	
$x = 0$	$x = 0.33$	$x = 0.44$	$x = 0.5$	$x = 0.66$	$x = 0.85$	$x = 1$	hkl	d	hkl	d	hkl	d
4.535	4.535	4.60	4.619				111	4.56	111	4.65		
2.760	2.797	2.84					220	2.80	220	2.846		
2.412	2.411	2.433	2.436				311	2.39	311	2.427		
2.270				2.405	2.403	2.420	222	2.28			111	2.410
			2.08	2.067								
1.961	1.996	2.017	2.026	2.012	2.078	2.081	400	1.977	400	2.013	200	2.088
1.518	1.531	1.549	1.555				511	1.520	511	1.5485		
			1.475	1.469								
1.393	1.416	1.425	1.432	1.424	1.470	1.473	440	1.395	440	1.4232	220	1.476
		1.22							533	1.2274		
			1.259		1.255	1.257			622	1.2134	311	1.259
					1.20	1.204	444	1.140	444	1.1613	222	1.206

[a] JCPDS table 10-425. [b] JCPDS table 10-339. [c] JCPDS table 4-0835.

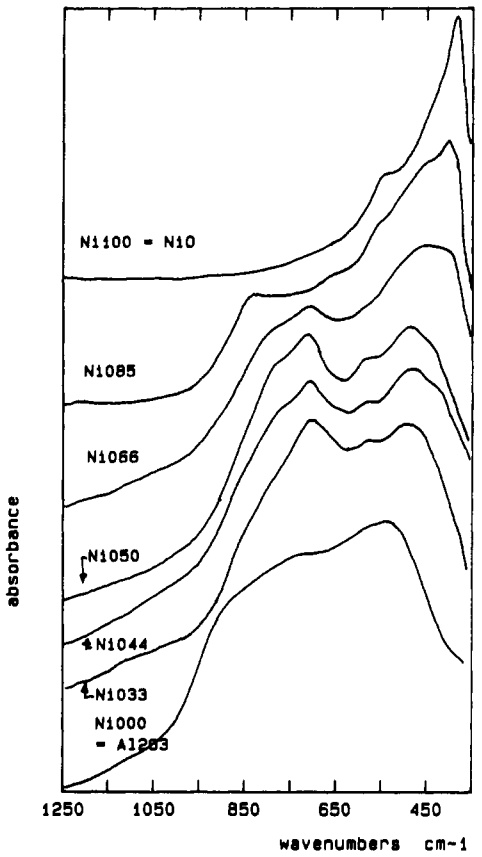

Figure 6. IR spectra (KBr pressed disks) of the $Ni_xAl_{2-2x}O_{3-2x}$ calcined powders.

investigated (Figure 6). The IR spectrum of Ni000 is consistent with that reported in the literature for γ-Al_2O_3,[30,31] although the IR spectra of transition aluminas are very sensitive to the thermal history of the samples. According to Tarte[32] the main maximum at 550 cm^{-1} is mainly associated with the vibrations of AlO_6 octahedra, while the very broad absorption extending from 950 to 700 cm^{-1} is associated with the vibrations of AlO_4 tetrahedra.[32-34] The broadness of all features in our spectra is due to the statistical nature of cation vacancy distribution both in octahedral and in tetrahedral sites for this phase.[17,30] The IR spectrum of Ni050, virtually identical to that of Ni050Na, is consistent with that reported for the inverse spinel $NiAl_2O_4$.[32] The main bands are at 730 and 505 cm^{-1}, with pronounced shoulders at 790 and 600 cm^{-1} and a weaker one near 880 cm^{-1}. The spectra of the Ni033 and Ni044 materials are very similar to those of the stoichiometric spinel, the band position being substantially identical, only the shoulder at 790 being strongly depressed in the sample Ni033.

According to literature data, the higher frequency one of the two stronger bands in spinels, generally found in the 1000–350-cm^{-1} region, is due to vibrations involving both octahedral and tetrahedral sites, while the lower frequency one only involves octahedra.[35] However, when the highest valency cation occupies tetrahedral sites, like in the inverse spinels, the highest frequency band should essentially be due to the vibration of the MO_4 tetrahedra.[36] In our case, we should conclude that the lowering of the lower frequency band from 550 cm^{-1} in alumina to 505 cm^{-1} in the Ni spinels as well as of the higher frequency band from near 850 to 730 cm^{-1} are related to the occupation of part of the octahedral sites by Ni^{2+}. The much better resolved spectrum of the Ni deficient spinels with respect to that of γ-alumina as well as the significant increase of the intensity of the higher frequency component are likely related to the better order in the distribution of cation vacancies, whose number decreases from 2.66 per 32 O^{2-} ions to 1.13 in Ni033 to 0.47 in Ni044, as well as to their preferential location in octahedral sites when Ni is present.

The IR spectrum of the pure reference material NiO is characterized by a main strong band at 405 cm^{-1}, with an evident shoulder at 560 cm^{-1} and a very weak one at 800 cm^{-1}, corresponding to the (110) and (100) transverse modes and to the longitudinal modes, respectively, in the rock salt structure.[37] The addition of Al^{3+} in the sample Ni085, that is also a monophasic although defective rock salt type structure according to XRD, results in the shift of the main maximum to 420 cm^{-1}, as well as in the appearance of new broad shoulders near 470 and 650 cm^{-1} and of a very evident band at 830 cm^{-1}. It seems very reasonable[32-34] to associate this latter feature to motions of AlO_4 tetrahedra and the feature near 470 cm^{-1} to AlO_6 octahedra. This spectrum seems to inequivocally show that Al^{3+} distributes between octahedral and tetrahedral sites in this structure. However, the different characteristics of the spectrum with respect to that of $NiAl_2O_4$ (Ni050) in the region 950–750 cm^{-1} support the idea that the tetrahedral Al^{3+} species do not arise from the spinel

(30) Baraton, M. I.; Quintard, P. *J. Mol. Struct.* **1982**, *79*, 337.
(31) Abbattista, F.; Delmastro, A.; Gozzelino, G.; Mazza, D.; Vallino, M.; Busca, G.; Lorenzelli, V. *J. Chem. Soc., Faraday Trans. 1* **1990**, *86*, 3653.
(32) Tarte, P. *Spectrochim. Acta* **1967**, *23A*, 2127.
(33) McKenzie, K. J. D. *J. Am. Ceram. Soc.*, **1972**, *55*, 68.
(34) Mazza, D.; Vallino, M.; Busca, G. *J. Am. Ceram. Soc.*, in press.
(35) Ishii, M.; Nakahira, M.; Yamanaka, T. *Solid State Commun.* **1972**, *11*, 209.
(36) Preudhomme, J.; Tarte, P. *Spectrochim. Acta* **1972**, *28A*, 69.
(37) Plendl, J. N.; In *Far Infrared Properties of Solids*; Mitra, S. S., Nudelman, S., Eds.; Plenum Press: New York, 1970; p 387.

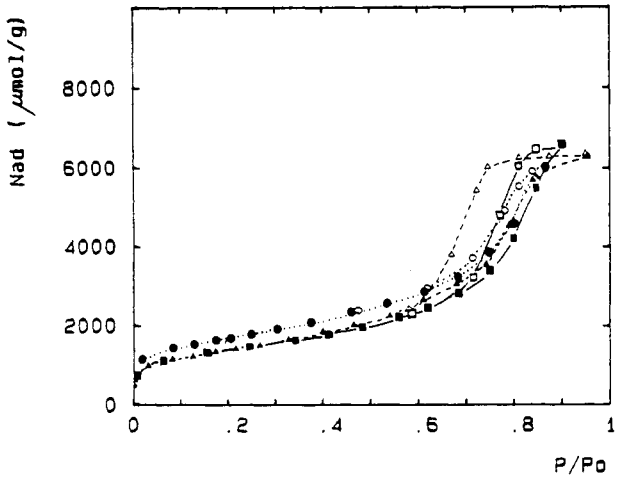

Figure 7. Nitrogen adsorption (closed symbols) and desorption (open symbols) isotherms at 77 K for Ni033 (squares), Ni050 (circles), and Ni085 (triangles).

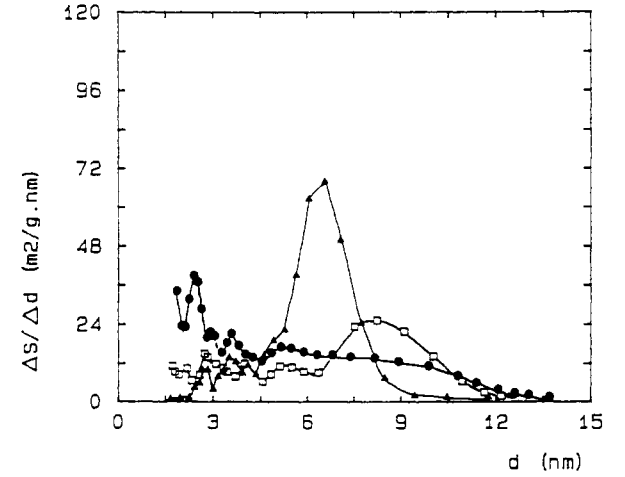

Figure 8. Pore distributions for Ni033 (squares), Ni050 (circles) and Ni085 (triangles). S = surface area; d = pore radius.

as a separate although minor phase. So, our data support the conclusion, already proposed by other authors,[13b,d,h] that this phase is a rock salt NiO-type phase with dissolved Al^{3+}.

(c) Microstructural Characterization. As reported in Table I, the surface area of all mixed oxides falls in the relatively sharp range 120 ± 13 m^2/g and is slightly higher than that of the pure oxides prepared by the same method. Also the crystal size, measured from XRD data, and the total pore volumes of all materials are very similar.

Figure 7 compares the nitrogen adsorption isotherms of three mixed oxide preparations (namely, Ni033, Ni050, and Ni085). The isotherms of Ni033 and Ni050 can be taken as typical of all other materials except Ni085. The isotherms of all powders are of type IV following the BDDT classification,[38] so providing evidence for the mesoporous nature of all materials under study. However, only in the case of Ni085 is a pronounced hysteresis found, probably related to the presence of ink-bottle pores. In the other cases cylindrical pores should predominate. The preparation of the stoichiometric spinel by precipitation with Na_2CO_3 does not differ significantly from that obtained using $(NH_4)_2CO_3$ also from this point of view.

Figure 8 shows the pore distribution curves of the same three materials. Again the Ni085 preparation differs slightly from the other for having a pronounced maximum, absent or much broader in all other materials.

Nevertheless, the porosity characterization data provides evidence for a strong similarity of all materials under study from the point of view of their microstructure, with only a very small deviation in the case of Ni085.

Table VI. Assignments of the IR Bands (cm^{-1}) Due to Surface Hydroxy Groups

notation	composition	$_{IV}$AlOH	$_{VI}$AlOH	NiOH	bridging	triply bridging
Ni000	γ-Al_2O_3	3790, 3770	3730		3680	3580
Ni033	def spinel	3790, 3770	3730		3680	3580
Ni044	def spinel	3790, 3770	3730		3680	3580
Ni050	$NiAl_2O_4$	3790	3730		3680	3580
Ni085	NiO-like	3790	3730		3680	
Ni100	NiO			3680	3600	

(d) Surface Hydroxy Groups. In Figure 9 the IR spectra in the OH stretching region of pressed disks of the pure powders after outgassing at 473 and 673 K are compared. The assignments of the observed bands to different types of free surface hydroxy groups are summarized in Table VI. They are based on our previous study[17] where we modified slightly the previous ones proposed by Knozinger and Ratnasami.[39]

The spectrum of the alumina sample, for which also the sample outgassed at 773 K is presented, compares well with those of a number of transitional alumina preparations.[39,17] The spectrum of the stoichiometric nickel aluminate has already been discussed by us.[17] The spectra of the nonstoichiometric spinels Ni033 (Figure 9) and Ni044 are similar to those of the stoichiometric spinel but show one more band at 3770 cm^{-1}, present also on spinel-type aluminas. This confirms our assignment of this band to a hydroxy group bonded to one tetrahedral aluminum ion placed near a cation vacancy, as occurs only in nonstoichiometric spinels.[17]

The comparison of the spectra of the hydroxy groups on the two stoichiometric $NiAl_2O_4$ preparations also allows to examine the effect of the precipitating agents, $(NH_4)_2CO_3$ or Na_2CO_3. The spectra are similar, although in the case of the sample obtained by precipitation with Na_2CO_3 the band at 3790 cm^{-1} is absent at all. The presence of slightly different amounts of a rock salt type phase in the preparations (definitely minor in both cases), that are not strictly speaking monophasic as discussed above, cannot justify apparently this effect. It seems likely that the groups responsible for this band, identified as OH groups bonded to one tetrahedral Al ion, are not present on Ni050Na being possibly their H^+ exchanged by Na^+ ions. The effect of the presence of Na^+ on the surface of nickel aluminate should be very similar to that caused on the surface of alumina, where both bands at 3790 and 3770 cm^{-1} are destroyed.[40]

The spectra of the biphasic material Ni066 and of the solid solution rock salt type oxide Ni085 are similar to that of $NiAl_2O_4$ (precipitation by $(NH_4)_2CO_3$)) although the band at 3680 cm^{-1} appears to grow and sharpen with increasing Ni content. Accordingly, NiO activated at 673 K presents only one sharp and intense band just at 3680 cm^{-1}, certainly due to hydroxy groups bonded to Ni^{2+} ions. On the basis of the assignments given in Table VI, the detection of the bands near 3790 and 3730 cm^{-1}, together with that at 3680 cm^{-1}, in the spectrum of the rock salt type solid solution oxide Ni085, indicates that on the surface of this material Al^{3+} cations are present, both in tetrahedral

(38) Gregg, S. J.; Sing, K. S. W. *Adsorption, Surface Area and Porosity*, 2nd ed.; Academic Press: New York, 1982.

(39) Knozinger, H.; Ratnasamy, P. *Catal. Rev.* **1978**, *17*, 31.

(40) Scokart, P. O.; Amin, A.; Defosse, C.; Rouxhet, P. G. *J. Phys. Chem.* **1981**, *85*, 1406.

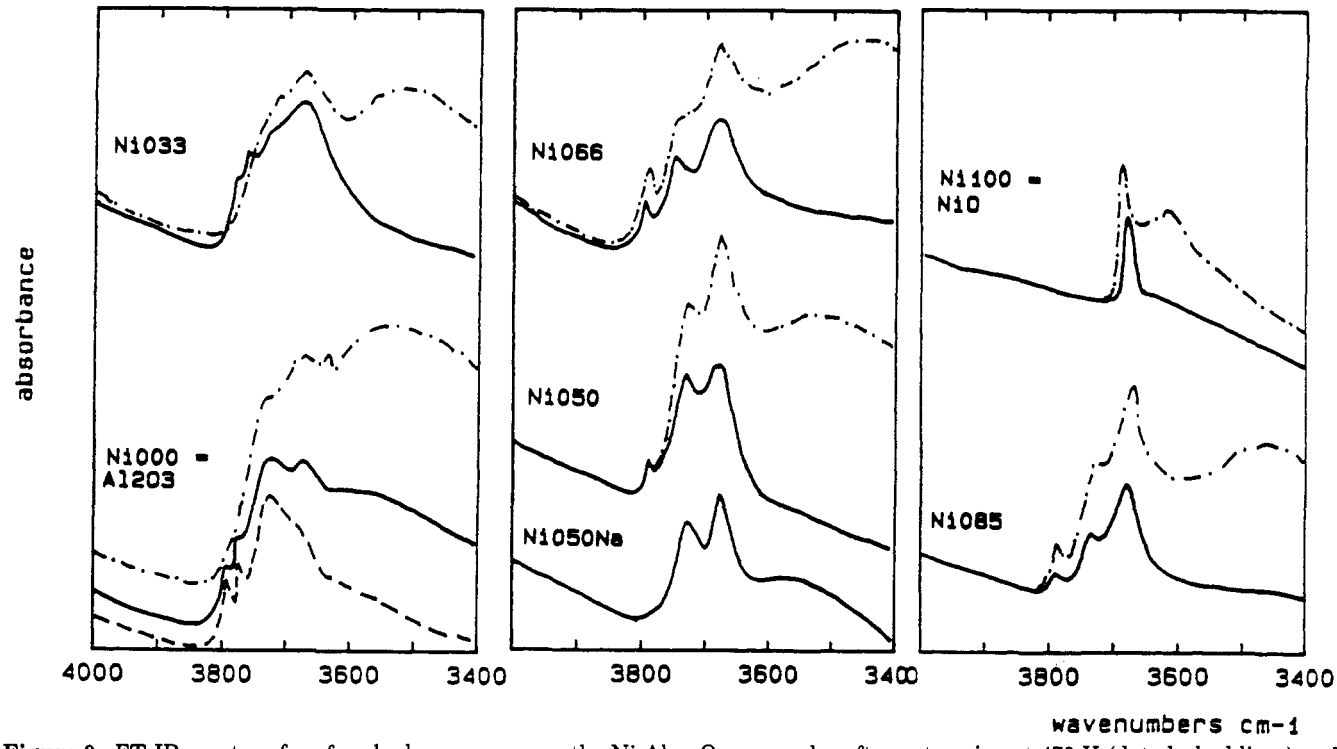

Figure 9. FT-IR spectra of surface hydroxy groups on the $Ni_xAl_{2-2x}O_{3-2x}$ samples after outgassing at 473 K (dot–dashed lines) and 673 K (full lines). Broken line: alumina outgassed at 773 K.

and in octahedral coordination, bonded to terminal hydroxy groups. This agrees with the conclusion arising from the skeletal IR spectrum of this powder, where features due to both AlO_4 tetrahedra and AlO_6 octahedra were found (see above).

The NiO spectra shown in Figure 9 appear to be closely related to those of other rock salt type binary oxides, namely, MgO (bands near 3750 and 3630 cm^{-1} (refs 41 and 42)) and CaO (bands near 3700 and 3610 cm^{-1} (refs 42 and 43)). Previously, Tsyganenko and Filimonov[42] reported a more complex spectrum for NiO possibly because of the presence of some impurity in their material.

(e) Surface Carbonyls Produced by Low-Temperature Carbon Monoxide Adsorption. Carbon monoxide can adsorb on the coordinatively unsaturated cationic or metallic centers on solid surfaces. The IR spectra of the resulting surface structures provide information on the coordinative and oxidative features of the adsorbing sites.[44] Low-temperature adsorption experiments also allow detection of weakly held surface carbonyls.

The spectra of CO adsorbed near 150 K on alumina (Figure 10) correspond to those reported recently by Zecchina et al.[45] The weak components observed near 2235 and 2210 cm^{-1} can be assigned to carbonyl species interacting with highly coordinatively unsaturated Al^{3+} ions, probably arising from tetrahedrally coordinated aluminum. The sharp band, detectable only at low temperature, whose maximum shifts from 2180 to 2200 cm^{-1} by evacuation (so by lowering the coverage) can be assigned to carbonyls over Al^{3+} centers in an overall octahedral coordination. Also the spectra recorded on the pure compound NiO (Figure 11) agree with literature data for high surface area nickel oxides. We observe a band, possibly having components both at higher and lower frequencies, near 2160 cm^{-1}, reasonably due to CO over Ni^{2+} in an unsaturated octahedral coordination.[46]

Table VII. Assignments of the IR bands (cm^{-1}) of Adsorbed CO Species

notation	composition	IV^{Al-CO}	VI^{Al-CO}	Ni–CO
Ni000	γ-Al_2O_3	2235, 2210	2180	
Ni033	def spinel	2210	2190	2160
Ni044	def spinel	2210	2190	2160
Ni050	$NiAl_2O_4$	2210	2190	2160
Ni085	NiO-like	2240		2170
Ni100	NiO			2160

The spectra observed on Ni033, Ni050 (Figure 10), and Ni066 (Figure 11) are similar to each other and can be interpreted on the basis of the assignments given above for pure oxides (Table VII). Two bands and a shoulder are observed that can be reasonably assigned to carbonyls on tetrahedral Al^{3+} (near 2210 cm^{-1}), on octahedral Al^{3+} (2190 cm^{-1}), and on Ni^{2+} (2160 cm^{-1}).

The spectrum observed on the sample Ni085 (Figure 11) again shows carbonyls on Al^{3+} in an overall tetrahedral coordination, although the frequency observed (2240 cm^{-1}) is higher in this case than in the cases of the other Ni-containing materials. Together, a strong band is observed near 2170 cm^{-1}, assigned to carbonyls over Ni^{2+}. Poor evidence is found for carbonyls over octahedral aluminum cations. The high frequency observed in this case for carbonyls over tetrahedral Al^{3+} and their apparent lower stability upon evacuation relative to carbonyls on nickel ions are features different with respect to those observed on the other Ni-containing powders. The structure of these sites cannot be determined on the basis of adsorbed CO only. We can only conclude that these sites have different geometries with respect to those of the spinel-type mate-

(41) Anderson, P. J.; Horlock, R. F.; Oliver, J. F. *Trans. Faraday Soc.* **1966**, *62*, 2754.
(42) Tsyganenko, A. A.; Filimonov, V. N. *Spectrosc. Lett.* **1972**, *5*, 477.
(43) Low, M. J. D.; Takezawa, N.; Goodsel, A. J. *J. Colloid Surf. Sci.* **1971**, *37*, 422.
(44) Nguyen, T. T.; Sheppard, N. In *Advances in Infrared and Raman Spectroscopies*; Clark, R. J. H., Hester, R. E., Eds.; Heyden: London, **1978**; Vol. 5, p 67.
(45) Zecchina, A.; Escalona-Platero, E.; Otero-Arean, C. *J. Catal.* **1987**, *107*, 244.
(46) Escalona-Platero, E.; Coluccia, S.; Zecchina, A. *Langmuir* **1985**, *1*, 407.

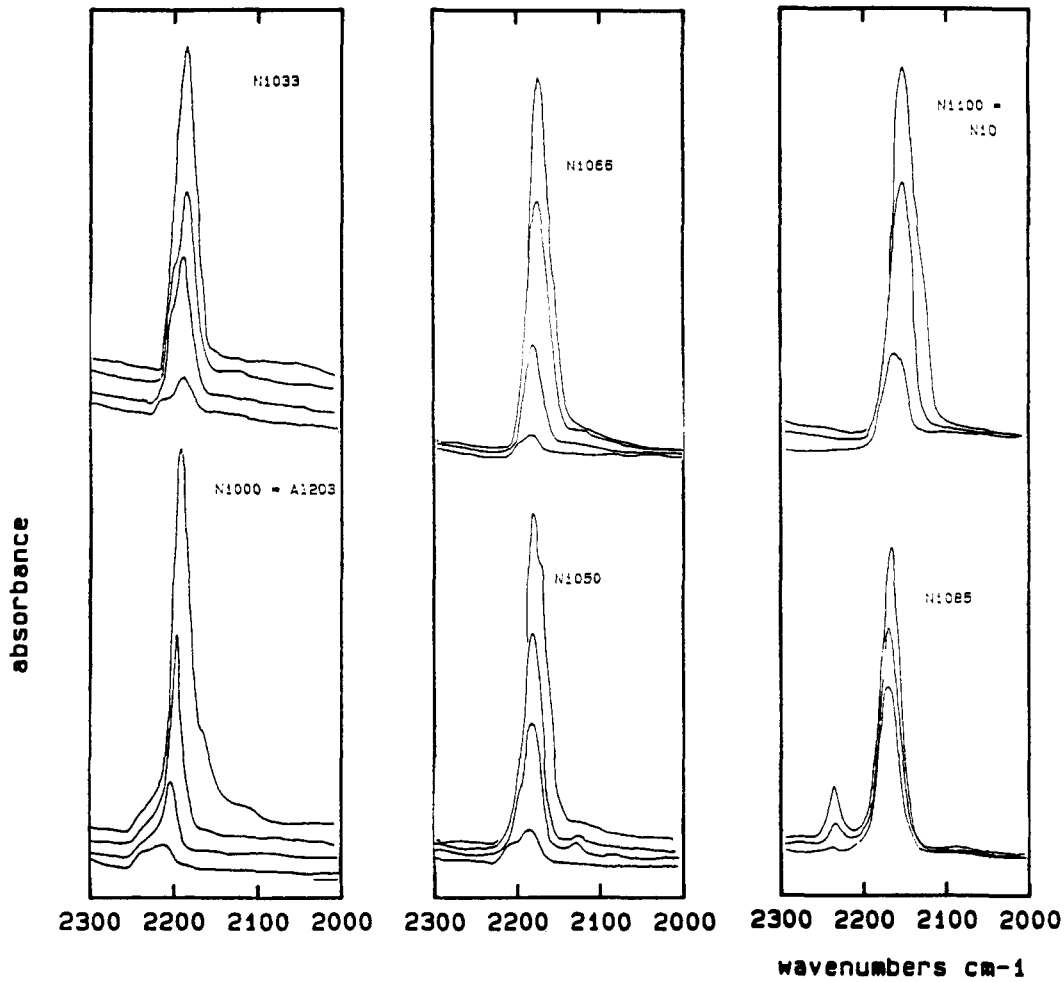

Figure 10. FT-IR spectra of CO adsorbed at 150 K on $Ni_xAl_{2-2x}O_{3-2x}$ samples (decreasing band intensity due to decreasing coverage by outgassing in the temperature range 150–220 K).

rials, so confirming again that tetrahedral Al^{3+} in the Ni085 sample does not arise from $NiAl_2O_4$ minor impurity.

(f) Surface Pyridine Complexes. In Figure 11 the spectra in the region 1700–1550 cm^{-1} of pyridine adsorbed on our materials are reported. In this region three bands are observable in liquid pyridine.[47] The most intense one, very sharp, is the 8a vibrational mode (1580 cm^{-1}), that is also the most sensitive one to coordination. In fact this band shifts upward the more, the stronger the Lewis site to which it coordinates. A weaker, sharp band, almost insensitive to coordination, is detected near 1575 cm^{-1} in the liquid (8b vibrational mode), while a combination mode (1+6a) can also be observed, weak and rather broad, near 1600 cm^{-1}. This combination, although sensititive to coordination, remains weak. So, only the behavior of the most intense 8a mode is discussed here. The assignments of the different bands arising from this mode of different surface complexes are summarized in Table VIII. They are based on the work of Morterra et al.[48] and on ourselves.[17]

The surface complexes arising from pyridine adsorption over Al_2O_3 are substantially the same as observed on other transitional aluminas as η-Al_2O_3[48] and δ-Al_2O_3.[17,49] The main modification when x grows from 0 to 0.5, going through defective spinels to the stoichiometric one, is the

Table VIII. Assignments of the IR Bands (cm^{-1}) of the 8a Mode of Adsorbed Pyridine

notation	composition	$_{IV}Al^{3+}$–py	$*_{IV}Al^{3+}$–py	Ni^{2+}–py	$_{VI}Al^{3+}$–py
Ni000	γ-Al_2O_3	1625	1615		1595
Ni033	def spinel	1625	1615	1605	1595
Ni044	def spinel	1625	1615	1605	1595
Ni050	$NiAl_2O_4$	1625		1605	1595
Ni085	NiO-like	1620		1604	
Ni100	NiO			1595	

[a] $*_{IV}Al^{3+}$–py = pyridine bonded over a tetrahedral Al^{3+} site placed near a cationic vacancy.

growth of a band at 1605 cm^{-1} (assigned to pyridine coordinated over Ni^{2+}) and the progressive disappearance of the band at 1615 cm^{-1}, (assigned accordingly to pyridine interacting with tetrahedral Al^{3+} placed near cation vacancies). So, the spectra recorded on Ni033 and on Ni044 provide a confirmation of our previous assignments.[17]

The spectrum of pyridine adsorbed on the Ni050Na surface is also reported in Figure 11 and can be compared with that of the corresponding Na-free compound. The spectra are significantly different: in fact, on the Na-containing material the band near 1625 cm^{-1} is not evident, while a component near 1585–1590 cm^{-1} is more prominent. The latter feature can be reasonably assigned to pyridine species interacting with Na^+ cations, being similar to the spectra observed on other alkali-metal-doped oxide surfaces.[50] From these data, it seems evident that the

(47) Corrsin, L.; Fax, B. J.; Lord, R. C. *J. Chem. Phys.* **1953**, *21*, 1170.
(48) Morterra, C.; Chiorino, A.; Ghiotti, G.; Garrone, E. *J. Chem. Soc., Faraday Trans. 1* **1979**, *75*, 271.
(49) Knozinger, H.; Krietenbrink, H.; Muller, H. D.; Schulz, W. In *Proc. 6th Int. Congr. on Catalysis*; The Royal Society of Chemistry: London, 1976; p 183.
(50) Busca, G.; Ramis, G. *Appl. Surf. Sci.* **1986**, *27*, 114.

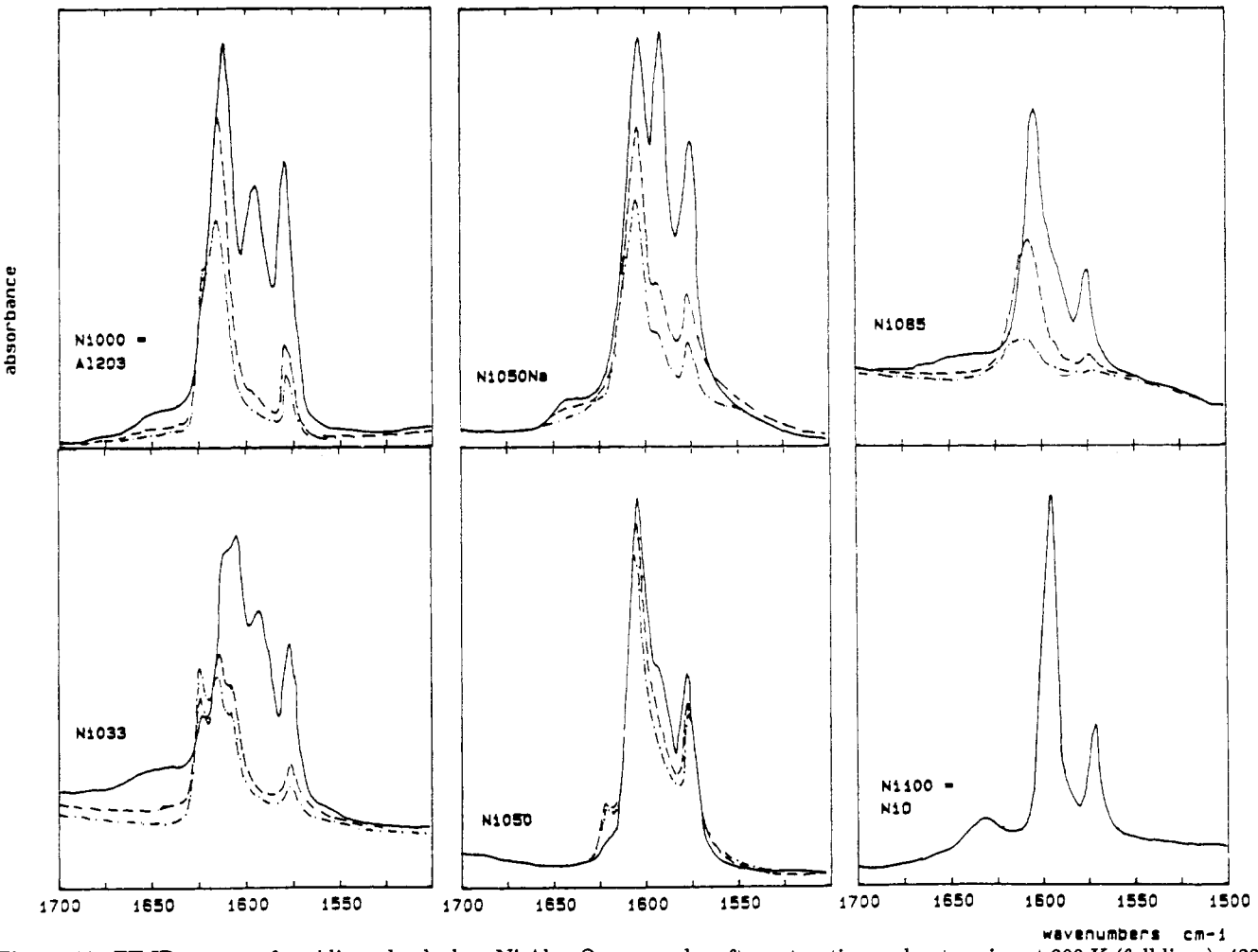

Figure 11. FT-IR spectra of pyridine adsorbed on $Ni_xAl_{2-2x}O_{3-2x}$ samples after saturation and outgassing at 300 K (full lines), 423 K (broken lines), and 473 K (dashed lines). On NiO heat treatment causes pyridine decomposition.

precipitation by sodium carbonate results in a sample where Al^{3+} ions in coordinatively unsaturated tetrahedral environment are not present, unlike on Na-free sample, and Na^+ cations are largely exposed on the surface.

The spectrum of pyridine adsorbed on NiO attests to the very poor acidity of this surface. In fact, only one chemisorbed species is found, whose spectrum is slightly perturbed with respect to that of free pyridine. Heat treatment of adsorbed pyridine on NiO even at so low a temperature as 373 K causes its chemical transformation, as already shown on other transition metal oxide surfaces.[51] It can be remarked that previously Tretyakov and Filimonov failed to observe pyridine coordination on NiO as well as on other basic rock salt type oxides as MgO and CaO.[52,53]

The spectrum of pyridine species on the Ni085 powder is significantly different from that detected on NiO, evidencing the strong perturbation of the acid–base and redox characters of the surface of NiO arising from the presence of Al^{3+}. In fact, a weak component is found near 1595 cm^{-1}, while the strongest band is at 1604 cm^{-1} but shifts to 1607 cm^{-1} by heating to 423 K. A shoulder also appears in these conditions near 1620 cm^{-1}, certainly due to species coordinated on surface tetrahedral aluminum cations. Pyridine is not transformed on the Ni085 surface even by heating to 473 K, according to a perturbation of the electronic structure of NiO when Al^{3+} is dissolved in it.

Conclusions

The data reported above show that high surface area mesoporous nickel aluminates can be prepared by coprecipitation from Ni–Al mixed nitrate water solutions followed by calcination in air. For $x < 0.5$ amorphous hydroxy nitrates are obtained that upon calcination decompose into Ni-deficient Ni–aluminate spinels. IR data suggest that these spinels are characterized by ordering of cation vacancies predominantly in octahedral sites. For $x = 0.5$, well-crystallized $NiAl_2O_4$ powders, with small amounts of a NiO-type phase impurity, are obtained irrespective from the precipitating agent $(NH_4)_2CO_3$ or Na_2CO_3. For $x > 0.5$, layered hydroxy carbonates and hydroxy nitrates carbonates are prepared, whose structures are similar to that of hydrotalcite. Calcination of these materials gives a rock salt type NiO phase including Al both in tetrahedral and in octahedral sites. Starting from solution having a Ni:Al atomic ratio = 3 ($x = 0.85$), the Ni analogue of hydrotalcite $Ni_6Al_2(OH)_{16}CO_3{\cdot}4H_2O$ is obtained that, by calcination, gives a monophasic rock-salt type compound having the formula $Ni_6Al_2O_9$.

The texture of the materials in the entire compositional range $0 \le Ni/Ni + Al \le 1$ is similar, and the surface areas high. In spite of the relatively high calcination temperature used by us (1073 K for 3 h), the surface areas of the mixed oxides so obtained are over 100 m^2/g, higher than those of the pure oxides prepared by the same method. In other words, nickel appears as a stabilizing agent toward alumina

(51) Busca, G.; Lorenzelli, V. *Mater. Chem.* **1981**, *6*, 175.
(52) Tretyakov, N. E.; Filimonov, V. N. *Kinet. Katal.* **1973**, *14*, 803.
(53) Tretyakov, N. E.; Filimonov, V. N. *Kinet. Katal.* **1970**, *11*, 989.

thermal sintering, besides adding new redox properties to it.

The IR studies of the surface hydroxy groups as well as of the surface complexes obtained by carbon monoxide and pyridine adsorption support and complete the criteria for the identification of surface sites on metal oxide surfaces, previously discussed by us,[17] arising from slight modifications of those of Knozinger and Ratnasami[39] for surface OH's and of Morterra et al. for Lewis acid sites.[48] In particular, it is confirmed that the presence of cationic vacancy clusters with respect to the spinel stoichiometry on the defective spinel aluminas and on bivalent-deficient aluminate spinels produces typical surface sites, absent on stoichiometric spinels.

IR data indicate that the surface composition of the mixed oxides $Ni_xAl_{2-2x}O_{3-2x}$ substantially reflects that of the bulk. In fact evidence of the presence at the surface of sites arising from all structures observed in the bulk has been provided. This is also the case of the Ni085 powder, found to be constituted by a monophasic rock salt type structure, whose unit cell is slightly contracted with respect to that of NiO as the result of the presence of relevant amounts of Al^{3+} in both tetrahedral and octahedral environments. The surface of this material is strongly modified with respect to that of pure NiO, showing complex νOH spectra and strong Lewis acid sites as the result of the presence of Al^{3+} ions in both tetrahedral and octahedral unsaturated coordination also at the surface. The higher thermal stability of pyridine adsorbed on it would also evidence a deep modification of its electronic properties with respect to NiO.

The present study also shows that $NiAl_2O_4$ prepared by sodium carbonate is contaminated by Na^+ ions at the surface, where tetrahedral Al^{3+} ions, responsible for strong Lewis acidity, are lacking or are poisoned. These sites are instead observed on samples prepared by ammonium carbonate coprecipitation.

Acknowledgment. The technical collaboration of R. Guidetti and C. Marcel is gratefully acknowledged. This work has been supported by MURST.

Registry No. $Ni_6Al_2(OH)_{16}(CO_3)\cdot 4H_2O$, 140468-28-6; Al_2O_3, 1344-28-1; $Ni_{0.33}Al_{1.34}O_{2.34}$, 140437-92-9; $Ni_{0.5}AlO_2$, 12004-35-2; $Ni_{0.85}Al_{0.3}O_{1.3}$, 140437-91-8; NiO, 1313-99-1; Na, 7440-23-5; CO, 630-08-0; boehmite, 1318-23-6; pyridine, 110-86-1; nitrogen, 7727-37-9; spinel, 12004-35-2.

Squaraine Chemistry. Design, Synthesis, and Xerographic Properties of a Highly Sensitive Unsymmetrical Fluorinated Squaraine

Kock-Yee Law

Xerox Webster Research Center, 800 Phillips Road, 0114-39D, Webster, New York 14580

Received October 29, 1991. Revised Manuscript Received February 17, 1992

A novel unsymmetrical fluorinated squaraine (UFSq), 3,4-dimethoxyphenyl-2′-fluoro-4′-(dimethylamino)phenylsquaraine, which was designed to improve the spectral sensitivity of squaraine in the visible region has been synthesized. The effects of synthesis and purification on the xerographic properties have been examined. Direct or indirect condensation of 1-(3′,4′-dimethoxyphenyl)-2-hydroxycyclobutene-3,4-dione with 3-fluoro-*N*,*N*-dimethylaniline affords UFSq in very similar chemical yields. The physical, morphological, and xerographic properties of UFSq samples from both routes are very similar also. Purification of UFSq by solvent extraction improves the purity of the as-synthesized UFSq samples. It was concluded, based on melting points and xerographic data, that CH_2Cl_2 extraction produces the "cleanest" sample for xerographic photoreceptor application. A bilayer device containing UFSq (CH_2Cl_2 purified) was shown to exhibit a low dark decay value (−15 V/s) and high panchromatic photosensitivity from the visible to the near-IR regions. The energies required to photodischarge half of the initial surface potential are 3.1 and 1.9 ergs/cm^2 at 600 and 790 nm, respectively. This sensitivity performance surpasses the sensitivity of all known squaraines and makes UFSq one of the most sensitive IR photoconducors known to date. Evidence is provided that the high sensitivity may be the result of the high purity and the high efficiency of hole injection of UFSq, from the charge generation layer to the charge-transporting layer, in the xerographic device. The electrical stability of UFSq is excellent. We have been able to show that the charging/photodischarging properties of an UFSq device remain unchanged after 50 000 cycles. This xerographic performance suggests that UFSq should be usable for diode laser (780 nm) and LED (660–680 nm) printers as well as copiers and multifunction printer-copiers.

Introduction

Bis(4-(dimethylamino)phenyl)squaraine (HSq) and many of its derivatives are organic photoconductors known to be usable in xerographic photoreceptors.[1,2] In solution, these compounds absorb at ~620–670 nm, depending on the substituent at the nitrogen and in the phenyl ring.[3] In the solid state, owing to the strong intermolecular donor–acceptor charge-transfer interactions, their absorptions

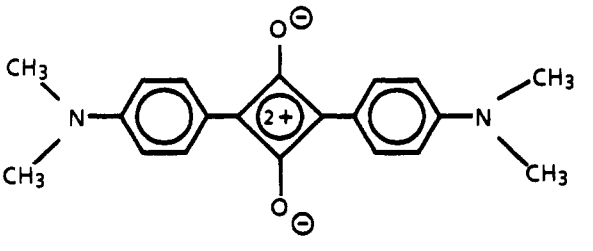

HSq

become very broad, typically exhibiting two bands, one in the visible region at 550–650 nm and the other in the

(1) Law, K. Y. *J. Imaging Sci.* **1987**, *31*, 83.
(2) Law, K. Y.; Bailey, F. C. *J. Imaging Sci.* **1987**, *31*, 172.
(3) Law, K. Y. *J. Phys. Chem.* **1987**, *91*, 5184.

0897-4756/92/2804-0605$03.00/0